

1 **The bacterial virulence factors rhamnolipids and their (R)-3-hydroxyalkanoate precursors activate**
2 ***Arabidopsis* innate immunity through two independent mechanisms**

3 Romain Schellenberger ^{a,1}, Jérôme Crouzet ^{a,1}, Arvin Nickzad ^b, Lin-Jie Shu ^c, Alexander Kutschera ^c, Tim Gerster ^c,
4 Nicolas Borie ^d, Corinna Dawid ^e, Maude Cloutier ^b, Sandra Villaume ^a, Sandrine Dhondt-Cordelier ^a, Jane Hubert ^d,
5 Sylvain Cordelier ^a, Florence Mazeyrat-Gourbeyre ^a, Christian Schmid ^e, Marc Ongena ^f, Jean-Hugues Renault ^d,
6 Arnaud Haudrechy ^d, Thomas Hofmann ^e, Fabienne Baillieul ^a, Christophe Clément ^a, Cyril Zipfel ^{g,h}, Charles Gauthier
7 ^b, Eric Déziel ^{b,2}, Stefanie Ranf ^{c,2} and Stéphan Dorey ^{a,2}

8
9 ^a Université de Reims Champagne-Ardenne, RIBP EA 4707, USC INRAE 1488, SFR Condorcet FR CNRS 3417, 51100, Reims,
10 France

11 ^b Centre Armand-Frappier Santé Biotechnologie, Institut national de la recherche scientifique (INRS), Laval, QC, H7V 1B7, Canada

12 ^c Phytopathology, TUM School of Life Sciences Weihenstephan, Technical University of Munich, Freising-Weihenstephan, 85354,
13 Germany

14 ^d Université de Reims Champagne-Ardenne, CNRS, ICMR 7312, SFR Condorcet FR CNRS 3417, 51097, Reims France

15 ^e Food Chemistry and Molecular Sensory Science, TUM School of Life Sciences Weihenstephan, Technical University of Munich,
16 Freising-Weihenstephan, 85354, Germany

17 ^f MiPI laboratory, SFR Condorcet FR CNRS 3417, Gembloux Agro-Bio Tech, University of Liège, Gembloux, B-5030, Belgium

18 ^g The Sainsbury Laboratory, University of East Anglia, Norwich Research Park, Norwich, NR4 7UH, UK

19 ^h Institute of Plant and Microbial Biology, Zurich-Basel Plant Science Center, University of Zurich, Zurich, Switzerland

20
21 ¹ These authors contributed equally to this work.

22 ² To whom correspondence may be addressed: E.D. (eric.deziel@inrs.ca) or S.R. (ranf@wzw.tum.de) or S.D. (stephan.dorey@univ-reims.fr).
23

24 **Classification:** biological sciences; plant biology

25 **Keywords:** plant immunity, rhamnolipids, HAA, *Pseudomonas*
26

27 **Abstract**

28 Plant innate immunity is activated upon perception of invasion pattern molecules by plant cell-surface immune
29 receptors. Several bacteria of the genera *Pseudomonas* and *Burkholderia* produce rhamnolipids (RLs) from L-
30 rhamnose and (R)-3-hydroxyalkanoate precursors (HAAs). RL and HAA secretion is required to modulate
31 bacterial surface motility, biofilm development, and thus successful colonization of hosts. Here, we show that
32 the lipidic secretome from the opportunistic pathogen *Pseudomonas aeruginosa*, mainly comprising RLs and
33 HAAs, stimulates *Arabidopsis* immunity. We demonstrate that HAAs are sensed by the bulb-type lectin
34 receptor kinase LIPOOLIGOSACCHARIDE-SPECIFIC REDUCED ELICITATION/S-DOMAIN-1-29
35 (LORE/SD1-29), which also mediates medium-chain 3-hydroxy fatty acid (mc-3-OH-FA) perception, in the
36 plant *Arabidopsis thaliana*. HAA sensing induces canonical immune signaling and local resistance to plant
37 pathogenic *Pseudomonas* infection. By contrast, RLs trigger an atypical immune response and resistance to
38 *Pseudomonas* infection independent of LORE. Thus, the glycosyl moieties of RLs, although abolishing
39 sensing by LORE, do not impair their ability to trigger plant defense. Moreover, our results show that the
40 immune response triggered by RLs is affected by the sphingolipid composition of the plasma membrane. In
41 conclusion, RLs and their precursors released by bacteria can both be perceived by plants, but through
42 distinct mechanisms.

43

44

45 **Significance**

46 Activation of plant innate immunity relies on the perception of microorganisms through self and non-self
47 elicitors. Rhamnolipids and their precursor HAAs are exoproducts produced by beneficial and pathogenic
48 bacteria. They are involved in bacterial surface dissemination and biofilm development. As these compounds
49 are released in the extracellular milieu, they have the potential to be perceived by the plant immune system.
50 Our work shows that both compounds independently activate plant immunity. We demonstrate that HAAs are
51 perceived by the receptor protein kinase LORE. By contrast, rhamnolipids are not sensed by LORE but
52 activate a non-canonical immune response influenced by the sphingolipid composition of the plant plasma
53 membrane. Thus, plants are able to sense bacterial molecules as well as their direct precursors to trigger
54 distinct immune responses.

55

56

57

58 Introduction

59 Plant innate immunity activation relies on detection of invasion pattern (IP) molecules that are
60 perceived by plant cells (1, 2). Non-self-recognition IPs include essential components of whole classes of
61 microorganisms, such as fragments of flagellin, peptidoglycans, mc-3-OH-FAs from bacteria or fragments of
62 chitin and β -glucans from fungi and oomycetes, respectively (3, 4). Apoplastic IPs are sensed by plant plasma
63 membrane-localized receptor kinases (RKs) or receptor-like proteins (RLPs) that function as pattern
64 recognition receptors (PRRs) (5, 6). Activation of the immune response requires the recruitment of regulatory
65 receptor kinases and receptor-like cytoplasmic kinases (RLCKs) by PRRs (7). Early cellular immune signaling
66 of pattern-triggered immunity (PTI) includes ion-flux changes at the plasma membrane, rise in cytosolic Ca^{2+}
67 levels, production of extracellular reactive oxygen species (ROS) and activation of mitogen-activated protein
68 kinases (MAPKs) and/or Ca^{2+} -dependent protein kinases (3, 8-10). Biosynthesis and mobilization of plant
69 hormones, including salicylic acid, jasmonic acid, ethylene, abscisic acid and brassinosteroids, ultimately
70 modulate plant resistance to phytopathogens (11-14).

71 Rhamnolipids (RLs) are extracellular amphiphilic metabolites produced by several bacteria, especially
72 *Pseudomonas* and *Burkholderia* species (15-17). Acting as wetting agents, RLs are essential for bacterial
73 surface dissemination called swarming motility and for normal biofilm development (18-20). These glycolipids
74 are produced from L-rhamnose and 3-(3-hydroxyalkanoyloxy)alkanoic acid (HAA) precursors (15, 21). HAAs
75 are synthesized by dimerization of (*R*)-3-hydroxyalkanoyl-CoA in *Pseudomonas*, forming congeners through
76 the RhIA enzyme (21). The opportunistic plant pathogen *Pseudomonas aeruginosa* and the phytopathogen
77 *Pseudomonas syringae* produce extracellular HAAs (16, 22-24). In *P. syringae*, HAA synthesis is coordinately
78 regulated with the late-stage flagellar gene encoding flagellin (22). HAA and RL production is finely tuned and
79 modulates the behavior of swarming migrating bacterial cells by acting as self-produced negative and positive
80 chemotactic-like stimuli (25). RLs contribute to the alteration of the bacterial outer membrane composition, by
81 shedding flagellin from the flagella (26) and by releasing lipopolysaccharides (LPS), resulting in an increased
82 hydrophobicity of the bacterial cell surface (27). In mammalian cells, RLs produced by *Burkholderia plantarii*
83 exhibit endotoxin-like properties similar to LPS, leading to the production of proinflammatory cytokines in
84 human mononuclear cells (28, 29). They also subvert the host innate immune response through manipulation
85 of the human beta-defensin-2 expression (30). Moreover, RLs from *Burkholderia pseudomallei* induce
86 Interferon gamma ($\text{IFN-}\gamma$)-dependent host immune response in goat (31).

87 In plants, RLs induce defense responses and resistance to biotrophic and necrotrophic pathogens (32,
88 33). They also contribute to the biocontrol activity of the plant beneficial bacterium *P. aeruginosa* PNA1
89 against oomycetes (17). Recently, it was reported that the bulb-type lectin receptor kinase
90 LIPOOLIGOSACCHARIDE-SPECIFIC REDUCED ELICITATION/S-DOMAIN-1-29 (LORE/SD1-29) mediates
91 medium-chain 3-hydroxy fatty acid (mc-3-OH-FA) sensing in *Arabidopsis thaliana* (hereafter, *Arabidopsis*) and
92 that bacterial compounds comprising mc-3-OH-acyl building blocks including LPS and RLs do not stimulate
93 LORE-dependent responses (34).

94 Here we show that the lipidic secretome produced by *P. aeruginosa* (RLsec), mostly composed of
95 RLs and HAAs, induces *Arabidopsis* immunity. HAAs are perceived through the RK LORE. We demonstrate
96 that, albeit not being sensed by LORE, RLs trigger an immune response characterized by an atypical defense

97 signature. Altogether, our results demonstrate that RLs and their precursors produced by *Pseudomonas*
98 bacteria stimulate the plant immune response by two distinct mechanisms.

99

100 Results

101 RLsec from *Pseudomonas* induces *Arabidopsis* immune responses partially mediated by LORE.

102 *Pseudomonas* species, including opportunistic plant pathogenic or plant beneficial endophytic strains, release
103 a mixture of RL congeners and HAA precursors, here collectively termed RL secretome (RLsec) (15, 25).
104 HPLC-MS/MS analyses of this RLsec from *P. aeruginosa* revealed the presence of mono-RLs and di-RLs at
105 50.9% and 44.9% of dry weight, respectively, and HAAs (3.8% of dry weight) (Supplementary Table 1,
106 Supplementary Fig.1). RLs comprising ten-carbon long lipid tails, Rha-C₁₀-C₁₀ (α -L-rhamnopyranosyl- β -
107 hydroxydecanoyl- β -hydroxydecanoate) and Rha-Rha-C₁₀-C₁₀ (α -L-rhamnopyranosyl- α -L-rhamnopyranosyl- β -
108 hydroxydecanoyl- β -hydroxydecanoate), and C₁₀-C₁₀ [(*R*)-3-(((*R*)-3-hydroxydecanoyl)oxy)decanoate] HAAs
109 were the most abundant molecules in this lipidic secretome (37.6%, 33.1%, 2.1%, respectively). Notably, low
110 amounts of free mc-3-OH-FAs (0.4% total), such as 3-OH-C₈, 3-OH-C₁₀ and 3-OH-C₁₂, were also identified
111 (Supplementary Table 1, Supplementary Fig.1).

112 First, we monitored apoplastic ROS production triggered by RLsec in *Arabidopsis* (35). Wild type (WT)
113 plants challenged with RLsec displayed a transient extracellular ROS production, starting at six minutes and
114 peaking at 15 minutes post elicitation (Fig. 1A). A robust ROS response was detected at concentrations of
115 RLsec starting from 0.5 μ g/mL (Fig. 1B, Supplementary Fig. 2). The ROS burst was dependent on the
116 transmembrane NADPH oxidase RBOHD (36, 37) (Fig. 1C, Supplementary Fig. 3). RKs and RLPs mediate
117 perception of IPs and early activation of PTI signaling (7). We monitored RLsec-triggered ROS production in
118 *Arabidopsis* plants carrying loss-of-function mutations in genes encoding well characterized RKs and RLPs
119 *fls2/efr1* (38, 39), *bak1-5*, *bkk1-1*, *bak1-5/bkk1-1* (40), *bik1/pbl1* (41), *cerk1-2* (42), *sobir1-12*, *sobir1-13* (43),
120 *dorn1-1* (44) and *lore-5* (45). RLsec-induced production of ROS was only reduced in *lore-5* (Fig. 1C,
121 Supplementary Fig. 3). Some IPs, including LPS extracts and mc-3-OH-FAs, were reported to induce a late
122 ROS production in *Arabidopsis* (34, 46, 47). The late ROS response triggered by mc-3-OH-FAs was
123 dependent on LORE (34). RLsec also induced a late and long-lasting ROS burst in *Arabidopsis* culminating at
124 6-8 hours post treatment (Fig. 2A), which was abolished in *rbohD* but not in *lore-5* mutant plants (Fig. 2A).

125 Next, we tested whether RLsec induces local resistance to the hemibiotrophic phytopathogen
126 *Pseudomonas syringae* pv. *tomato* DC3000 (*Pst*) in *Arabidopsis* (48). RLsec pretreatment significantly
127 enhanced resistance against *Pst* infection in WT and *lore-5* plants (Fig. 2B). Taken together, our results show
128 that RLsec induces immunity-related signaling events and disease resistance in *Arabidopsis* that are partially
129 mediated by the bulb-type lectin RK LORE.

130

131 *Pseudomonas* HAAs and mc-3-OH-FAs from RLsec trigger LORE-dependent *Arabidopsis* immunity.

132 By contrast to RLsec, purified RLs do not trigger LORE-dependent [Ca²⁺]_{cyt} and early ROS signaling
133 responses (34). Because RLsec contains significant amounts of HAAs, we investigated the role of these
134 poorly studied compounds in RLsec-triggered immunity. We compared the responses to HAA with those to
135 mc-3-OH-FAs, known to be sensed by LORE (34) and present in low amounts in RLsec (Supplementary table
136 1). Side-by-side experiments with C₁₀-C₁₀ HAA purified from *Pseudomonas aeruginosa* secretome and 3-OH-

137 C₁₀ revealed that both compounds induce [Ca²⁺]_{cyt} signaling and ROS production in *Arabidopsis* plants in a
138 dose-dependent manner (Fig. 3A and 3B, Supplementary Fig. 4 and 5). As observed upon 3-OH-C₁₀
139 elicitation, purified C₁₀-C₁₀-induced ROS response was impaired in *rbohD* and *lore-5* mutants (Fig. 3C).
140 Similarly, [Ca²⁺]_{cyt} signaling triggered by C₁₀-C₁₀ was impaired in *lore-5* (Fig. 3D). In addition, C₁₀-C₁₀ and 3-
141 OH-C₁₀ both triggered LORE-dependent MPK3 and MPK6 phosphorylation (Supplemental Fig. 6A). WT but
142 not *lore-5* mutant plants pretreated with C₁₀-C₁₀ or 3-OH-C₁₀ displayed enhanced resistance against *Pst* (Fig.
143 3E). Similar to 3-OH-FAs (34), the acyl chain length of HAA affects its immune eliciting activity, as purified
144 C₁₄-C₁₄ from *B. glumae* did neither induce ROS production nor enhanced resistance to *Pst* in *Arabidopsis*
145 plants (Supplementary Fig. 7A and B).

146 Trace amount of 3-OH-C₁₀ was detected in C₁₀-C₁₀ purified from *P. aeruginosa* RLsec (Supplementary
147 Table 2). To avoid any influence of potential contamination of HAAs with eliciting compounds related to
148 purification procedure, we tested chemically synthesized C₁₀-C₁₀ for the ROS and [Ca²⁺]_{cyt} responses.
149 Synthetic C₁₀-C₁₀ triggered LORE-dependent [Ca²⁺]_{cyt} signaling and ROS production in a dose-dependent
150 manner (Fig. 4A-C). WT plants pretreated with synthetic C₁₀-C₁₀ also displayed LORE-dependent enhanced
151 resistance against *Pst* infection (Fig. 4D). LORE binds 3-OH-C₁₀ through its extracellular domain (eLORE)
152 (34). In a ligand depletion assay (Supplementary Fig. 8A), synthetic C₁₀-C₁₀ was depleted from the low-
153 molecular-weight fraction after size-exclusion filtration when incubated with eLORE-mCherry fusion protein
154 transiently expressed in the apoplast of *Nicotiana benthamiana*, but not upon incubation with an apoplastic
155 mCherry control, similarly as observed for the 3-OH-C₁₀ ligand (Fig. 4E, Supplementary Fig. 8) (85). This
156 strongly suggests binding of C₁₀-C₁₀ to eLORE.

157 Altogether, our results show that HAAs secreted by *Pseudomonas* are sensed by *Arabidopsis* through
158 the bulb-type lectin RK LORE, activate canonical PTI-related immune responses and provide resistance to
159 bacterial infection.

160

161 **RLs trigger LORE-independent *Arabidopsis* immune responses and resistance to *Pst*.**

162 To investigate whether RLs activate a LORE-independent immune response, we used purified Rha-
163 Rha-C₁₀-C₁₀ and Rha-C₁₀-C₁₀, the most abundant molecules from *P. aeruginosa* RLsec. In *Arabidopsis* WT,
164 both RL congeners induced a late and long-lasting ROS production, but as observed previously (34), no early
165 burst (Fig. 5A). As both RL congeners gave a similar ROS signature, we only used Rha-Rha-C₁₀-C₁₀ in the
166 following experiments. The minimal concentration necessary to stimulate ROS production was 50 μM with an
167 optimum at 100 μM (Fig. 5B). Late ROS production was compromised in *rbohD* but not in *lore-5* mutants (Fig.
168 5C). Surprisingly, neither MPK3 nor MPK6 activation by Rha-Rha-C₁₀-C₁₀ was detectable over a 3-hour time-
169 course (Supplementary Fig. 6A and B). L-Rhamnose alone was inactive demonstrating that the lipid part of the
170 RLs is necessary to trigger the immune response (Fig. 5A). *Burkholderia* species produce RL congeners with
171 longer lipid chains than those produced by *Pseudomonas* (15). The RLsec from phytopathogenic *Burkholderia*
172 *glumae* only contains congeners with fatty acid chain lengths varying from 12 to 16 carbons, in particular Rha-
173 Rha-C₁₄-C₁₄ (49, 50). Challenge of *Arabidopsis* with purified Rha-Rha-C₁₄-C₁₄ from *B. glumae* did not trigger
174 any ROS production (Fig. 5A) suggesting that the length of the fatty acid chain of RLs is critical for their
175 eliciting activity. To determine whether RLs trigger local resistance to pathogenic *Pseudomonas* independent

176 of LORE, plants were pretreated with 10 μ M purified Rha-Rha-C₁₀-C₁₀ before *Pst* inoculation. WT plants
177 displayed a significant enhanced resistance against *Pst* that was not compromised in *lore-5* mutants (Fig. 5D).

178 To get deeper insights into the mechanisms involved in RL sensing, we used *Arabidopsis* plants
179 carrying loss-of-function mutations in genes encoding RK and RLPs but also plasma membrane channel
180 mutants including quintuple mechano-sensitive channels of small conductance-like (*msl4/5/6/9/10*) and double
181 mid1-complementing activity (*mca1/2*) channel mutants (51) that could monitor changes in membrane
182 mechanical properties. None of these mutants were affected in the long-term ROS response (Fig. 6A).
183 Glycosylinositol phosphorylceramide (GIPC) sphingolipids were recently involved in the sensing of microbial
184 necrosis and ethylene-inducing peptide 1-like (NLP) proteins (52). We found that the fatty acid hydroxylase
185 *fah1/2* mutant that is disturbed in its complex sphingolipid composition (52) showed a reduced long-term ROS
186 response (Fig. 6B). Ion leakage measurement confirmed that *fah1/2* mutant plants were less affected than WT
187 plants by RL treatment (Fig. 6C). *fah1/2* plants are known to be more resistant to obligate biotrophic
188 pathogens (86). We also observed that these mutants were more resistant to *Pst* (Fig. 6D). However, unlike in
189 WT plants, challenge of *fah1/2* with RLs did not triggered enhanced resistance to *Pst* in the mutants,
190 confirming that RL-triggered responses are compromised in these plants (Fig. 6D). Ceramide synthase *loh1*
191 mutants are also impaired in GIPC levels but not in glucosyl ceramides (52). Interestingly, RL-triggered ROS
192 production and ion leakage was unaltered in *loh1* plants. Altogether, our results show that RLs activate an
193 atypical immune response in *Arabidopsis* that is LORE-independent, but which is affected by the sphingolipid
194 composition of the plasma membrane.

195

196 Discussion

197 In *Pseudomonas* and *Burkholderia* species, swarming motility is intimately related to the production of
198 extracellular surface-active RLs and HAAs (22, 25, 53-55). In addition, RL production affects bacterial biofilm
199 architecture and increases affinity of cells for initial adherence to surfaces through increasing the cell's surface
200 hydrophobicity (19, 56). These exoproducts are therefore at the frontline during host colonization. Our work
201 demonstrates that both RLs and HAAs from the *Pseudomonas* lipidic secretome, referred to as RLsec here,
202 are able to trigger *Arabidopsis* innate immunity by two distinct mechanisms.

203 We found that *Pseudomonas* RLs induce an atypical immune response. This response does not
204 involve the RK LORE. Other bacterial compounds comprising mc-3-OH-acyl building blocks, but with large
205 decorations including lipid A or LPS, lipopeptides, and *N*-acyl homoserine lactones also do not trigger LORE-
206 dependent immune responses (34). RLs are glycolipids made of L-rhamnose linked to an HAA lipid tail (15,
207 21). Therefore, we propose that glycosylation of HAAs abolishes their perception by LORE. Glycosylation is
208 known to affect the perception of IPs. Glycosylation of the flagellin from *Acidovorax avenae* on Ser¹⁷⁸ and
209 Ser¹⁸³ prevents its perception by rice cells (57). Similarly, unglycosylated flagellin from *Pseudomonas syringae*
210 pv. *tabaci* 6605 induces stronger defense responses in tobacco plants than glycosylated flagellin (58). In
211 humans, glycosylation of *Burkholderia cenocepacia* flagellin significantly reduces its perception by epithelial
212 cells (59).

213 We found that RL perception does not involve previously characterized RKs, RLPs or
214 mechanosensitive channels. However, the RL response is affected by alterations in sphingolipid synthesis
215 suggesting a role of these key membrane lipids in RL-triggered immunity. Recently GIPCs, major structural

216 components of the plant plasma membrane together with glucosylceramides (GlcCers), have been involved
217 as receptors of cytotoxic NLPs (52). NLPs bind terminal monomeric hexose moieties of GIPCs. Only eudicot
218 plants are sensing these NLPs through sphingolipid receptors. Insensitivity of monocots to NLPs is due to the
219 length of the GIPC headgroup, consisting of three terminal hexoses compared to two in eudicots (52). *fah1/2*
220 mutants display reduced glycosylsphingolipid (GIPCs and GlcCers) content but also lower level of ordered
221 plasma membranes (52), suggesting that, similar to the NLP response, complex sphingolipids and/or ordered
222 plasma membranes are necessary for the RL response. Unlike NLPs, RL responses were not significantly
223 affected in *loh1* mutant plants also suggesting that GlcCers more than GIPC could influence RL sensing (52).
224 Surfactin and more recently synthetic RL bolaforms and synthetic glycolipids, also active in the micromolar
225 range, have been proposed to directly interact with plasma membrane lipids (46, 60-62). Mono- and di-RLs
226 from *Pseudomonas* interact with phospholipids in several model membranes (63-66). In particular, RLs are
227 able to fit into phospholipid bilayers of plant membrane models (67). In this model, the rhamnose polar heads
228 from RLs are located near the phosphate groups from phospholipids and RL hydrophobic lipid tails are
229 surrounded by the lipid chains from these phospholipids (67). The results obtained with these plant plasma
230 membrane models suggest that the insertion of RLs into the lipid bilayer does not significantly affect lipid
231 dynamics. The nature of the phytosterols could however influence the RL effect on plant plasma membrane
232 destabilization. Subtle changes in lipid dynamics could then be linked to plant defense induction (67).
233 Interestingly, RL bolaforms, like natural RLs are inducing a non-canonical defense signature with a long-
234 lasting oxidative burst without MPK3 or MPK6 activation (46). We showed that the late ROS response
235 triggered by RLs and RL-bolaforms is fully dependent on RBOHD which differs from the second ROS
236 response observed after LPS treatment and produced by chloroplasts (47). The RL-related ROS response is
237 not directly linked to *Arabidopsis* protection to *Pst* as some bolaforms can trigger this late ROS production
238 without increasing resistance to *Pst* (46). However, the experiments from Luzuriaga et al. and our results on
239 natural RLs suggest that the late ROS response is closely linked to ion leakage and may therefore be involved
240 in membrane destabilization. This atypical defense signature triggered by two structurally different RLs,
241 displaying amphiphilic properties and biological activities at the micromolar range, may suggest a direct
242 interaction of these molecules with plant plasma membrane lipids, similar to what has been shown on
243 membrane models (46).

244 We also demonstrated that HAAs, found in large amount in *Pseudomonas* lipidic secretome, are IPs
245 perceived by *Arabidopsis*. HAA sensing is mediated by LORE. HAAs, in the micromolar range, induce typical
246 PTI responses including transient ROS production, $[Ca^{2+}]_{cyt}$ signaling, and MPK3 and MPK6 phosphorylation
247 in *Arabidopsis*. Interestingly, 3-OH-C₁₀ activates similar responses but at concentrations 10 to 50 times lower.
248 This is intriguing, because HAAs are present in much larger quantities (more than 3%) compared to 3-OH-FAs
249 (0.3%) in the lipidic secretome (Supplemental table 1). This high amount of HAAs may compensate for their
250 lower activity. RLs are activating an immune response at relatively high concentrations compared to both
251 compounds. Interestingly, the RL concentration in the *P. aeruginosa* lipidic secretome is 10 to 100 times
252 higher than HAAs and usually is in the millimolar range (23, 68). RLs are produced between 20 and 110 μ M *in*
253 *vivo* in mammals infected by *P. aeruginosa*, especially during cystic fibrosis disease (69-71). The high
254 concentrations of RLs needed for plant elicitation are in the range of the concentrations produced by the
255 bacteria.

256 Higher steric hindrance of HAA compared to 3-OH-FAs likely results in a lower affinity to the LORE
257 receptor. Synthetic ethyl 3-hydroxydecanoate (Et-3-OH-C10:0) and *n*-butyl 3-hydroxydecanoate (*n*But-3-OH-
258 C10:0), which possess unbranched ester-bound carbon chains in place of the carboxyl group, also triggered
259 LORE-dependent immune signaling in *Arabidopsis*, while 3-branched *tert*-butyl 3-hydroxydecanoate (*t*But-3-
260 OH-C10:0) was inactive (34). HAAs, possessing a 2-branched ester-bound headgroup, activate LORE
261 signaling. The differences in efficacy could be explained by the different steric hindrance of the molecules.
262 Alternatively, the additional carboxyl group could account for the LORE-eliciting activity of HAAs.

263 *Pantoea*, *Dickeya* and *Pseudomonas* bacteria, in particular the well-known phytopathogen *P. syringae*
264 mainly produce HAAs containing 3-hydroxydecanoic acid (C₁₀) tails (15, 22, 72). By contrast, *Burkholderia*
265 species including the phytopathogenic bacterium *B. glumae*, mainly produce HAAs comprising 3-
266 hydroxytetradecanoic acid (C₁₄) tails (49). *Pseudomonas* C₁₀-containing HAAs activated *Arabidopsis* PTI
267 whereas *Burkholderia* HAAs containing C₁₄ fatty acid did not. Chain-length specificity was also observed for
268 mc-3-OH-FA sensing by the LORE receptor with 3-OH-C₁₀ representing the strongest immune elicitor (34).
269 Thus, it could be hypothesized that *Arabidopsis*, and more generally *Brassicaceae* (73), are able to
270 specifically recognize HAAs from specific bacterial species, among which several are plant opportunistic and
271 phytopathogens (74-77). Interestingly, transcript profiles of the bean pathogen *P. syringae* pv. *syringae* B728a
272 support a model in which leaf surface or epiphytic sites specifically favor swarming motility based on HAA
273 surfactant production (55, 78). Low levels of HAAs contributing to motility are produced by these bacteria (22).
274 HAA concentrations necessary to stimulate *Arabidopsis* innate immunity are in line with the concentration
275 detected in RLsec and are produced by *Pseudomonas* (between 3 to 20% of the secretome) (23, 68, 79).

276 Low amounts of free mc-3-OH-FAs were found in RLsec from *P. aeruginosa* (Supplementary table 1).
277 In *Pseudomonas*, the outer membrane lipase PagL releases 3-OH-C₁₀ during synthesis of penta-acylated lipid
278 A (34). The further fate of this 3-OH-C₁₀ is unknown. RLs are able to extract LPS from the outer membrane of
279 *P. aeruginosa* (27). Conceivably, surface-active RLs, and presumably also HAAs, could release free 3-OH-C₁₀,
280 produced through PagL activity, along with LPS from the bacterial cell wall or outer membrane vesicles (27).
281 Alternatively, degradation of HAAs/RLs *in planta* may also release free 3-OH-C₁₀. Acyl carrier protein (ACP)-
282 and coenzyme A (CoA)-bound mc-3-OH-FAs are precursors of HAA/RL synthesis (21). Upon bacterial cell
283 lysis, enzymatic or non-enzymatic degradation processes may also generate free 3-OH-C₁₀ from these
284 precursors. *In vivo*, insights into IP release have been recently obtained for flagellin. The plant glycosidase
285 BGAL1 facilitates the release of immunogenic peptides from glycosylated flagellin, upstream of cleavage by
286 proteases (80). The pathogen may evade detection by altering flagellin glycosylation and inhibiting the plant
287 glycosidase. Flagellin glycosylation increases its physical stability that could contribute to the non-
288 liberation/recognition of the flg22 epitope (58, 81). RLs are able to shed flagellin from *P. aeruginosa* flagella
289 (26), suggesting that these biosurfactants participate in the release of this and presumably other eliciting
290 compounds.

291 In conclusion, we hypothesize that when HAA- and RL-producing *Pseudomonas* colonize the leaf or
292 root surface, they release RLs and HAAs which are necessary for surface motility, biofilm development, and
293 thus successful colonization. Whereas *Arabidopsis* senses HAAs and mc-3-OH-FAs through the bulb-type
294 lectin receptor kinase LORE, RLs are perceived through a LORE-independent mechanism (Figure 7). In

295 addition to direct activation of a non-canonical defense response in plants, RLs, by releasing other IPs from
296 bacteria, could orchestrate a node leading to strong activation of plant immunity.

297

298

299 **Methods**

300 **Molecules.** The *P. aeruginosa* lipidic secretome used in this study was obtained from Jeneil Biosurfactant Co.,
301 Saukville, USA (JBR-599, lot. #050629). Rha-Rha-C₁₀-C₁₀ and Rha-C₁₀-C₁₀ were purified from this lipidic
302 secretome mixture, as previously described (33, 34). Rha-Rha-C₁₄-C₁₄ were purified from the *B. glumae* lipidic
303 secretome (49). To obtain pure HAAs from *P. aeruginosa* or *B. glumae*, RLs were hydrolyzed using 1 M HCl
304 in 1:1 dioxane-water boiling at reflux for 60 min. The mixture was extracted with ethyl acetate and the extracts
305 were dried over anhydrous Na₂SO₄. After filtration, the resulting extracts were then evaporated to dryness and
306 resuspended in 2 mL of methanol. HAAs were then isolated from digested mixture using flash
307 chromatography on a Biotage (Stockholm, Sweden) Isorela One instrument with a SNAP Ultra C18 12g
308 column (Biotage) using an acetonitrile/water gradient at 12 mL/min flow rate. The elution was started with 0%
309 acetonitrile for 4.5 min and the acetonitrile concentration was raised to 100% over 28.2 min, followed by an
310 isocratic elution of 100% acetonitrile for 13.3 min. The flash chromatography fraction containing the C₁₀-C₁₀
311 was further separated and purified using 0.25 mm thin-layer chromatographic (TLC) plates (SiliCycle
312 SilicaPlate F-254) and developed with *n*-hexane-ethyl acetate-acetic acid (24:74:2). The bands were scraped
313 from the plates and the HAAs, including C₁₀-C₁₀, were extracted from the silica with chloroform-methanol (5:1).
314 3-OH-C₁₀ was purchased from Sigma-Aldrich Saint-Quentin Fallavier, France. All compounds were dissolved
315 in ethanol or methanol as indicated to prepare stock solutions. Final aqueous compound dilutions were
316 prepared freshly on the days of the experiment. Control solutions contained equal amounts of ethanol or
317 methanol (0.05% for most experiments and not exceeding 0.5% for the highest concentrations tested).
318 Chemical synthesis of C₁₀-C₁₀ is described in Datasets S1 and S2.

319

320 **LC-MS analysis of HAAs.** Samples were prepared by diluting stock solutions using MeOH to final
321 concentration of 50 ppm. 16-Hydroxyhexadecanoic acid at 20 ppm was added to samples as internal
322 standard⁷¹. The analyses were performed with a Quattro II triple quadrupole mass spectrometer (Micromass,
323 Pointe-Claire, Canada) equipped with a Z-spray interface using electrospray ionization in negative mode. The
324 capillary voltage was set at 3.5 kV and the cone voltage at 25 V. The source temperature was kept at 120°C
325 and the desolvation gas at 150°C. The scanning mass range was from 130 to 930 Da. The instrument was
326 interfaced to a high-performance liquid chromatograph (HPLC; Waters 2795, Mississauga, Ontario, Canada)
327 equipped with a 100 x 4 mm i.d. Luna Omega PS C18 reversed-phase column (particle size 5 µm) using a
328 water-acetonitrile gradient with a constant 2 mmol L⁻¹ concentration of ammonium acetate (0.6 mL.min⁻¹).
329 Quantification of free 3-OH-C₁₀ in purified C₁₀-C₁₀, Rha-Rha-C₁₀-C₁₀, Rha-C₁₀-C₁₀, Rha-Rha-C₁₄-C₁₄ or
330 synthetic C₁₀-C₁₀ were performed as reported previously (34) and are presented in Supplementary table 2.

331

332 **Plant material and growth conditions.** *Arabidopsis thaliana* ecotype Col-0 was used as WT parent for all
333 experiments. Seeds from *fls2/efr1* (38, 39), *bak1-5*, *bkk1-1*, *bak1-5/bkk1-1* (40), *cerk1-2* (42), *bik1/pbl1* (41),
334 *rbohD*, *msl4/5/6/9/10* and *mca1/2* (51) were provided by C. Zipfel. Seeds from *sobir1-12* and *sobir1-13* (43)

335 were provided by F. Brunner (*Center for Plant Molecular Biology, University of Tübingen, Tübingen,*
336 *PlantResponseTM*). Seeds from *sd1-29 (lore-5)*, Col-0^{AEQ} and *lore-5^{AEQ}* were provided by S. Ranf (45). *loh1*
337 and *fah1/2* seed (52) were provided by I. Feussner (*University of Göttingen, Germany*). *dorn1-1* seeds (44)
338 were obtained from NASC stock (SALK_042209). All mutants are in the Col-0 background. Plants were grown
339 on soil in growth chambers at 20°C, under 12 h light / 12 h dark regime with fluorescent light of 150 $\mu\text{mol m}^{-2}$
340 s^{-1} and 60% relative humidity.

341

342 **Extracellular ROS production and calcium signaling.** ROS assays were performed on 4- to 6-week-old
343 *Arabidopsis* plants cultured on soil. Briefly, 5 mm long petiole sections were cut and placed in 150 μL of
344 distilled water overnight in 96 wells plate (PerkinElmer) (46). Then, the protocol was conducted as previously
345 described (82). Luminescence (relative light units, RLU) was measured every 2 min during 46 or 720 min with
346 a Tecan Infinite F200 PRO (or a TECAN CM SPARK for Supplementary figure 6), Tecan France. Total ROS
347 production was calculated by summing RLU measured between 4 to 46 or 4 to 720 minutes after treatment.
348 Control was realized on petioles of WT or mutant plants. $[\text{Ca}^{2+}]_{\text{cyt}}$ measurements were done as previously
349 described (34).

350

351 **MAPK phosphorylation assays.** For MAPK phosphorylation assays, 3 leaf disks (9 mm diameter) were
352 collected from 4 to 6-week-old *Arabidopsis* plants grown on soil and incubated 8 h in distilled water. Leaf disks
353 were mock-treated or treated with different molecules. 15 min, 1 hour, and 3 hours after treatment, plant
354 tissues were frozen in liquid nitrogen. To extract proteins, 60 mg of leaf tissues were ground in a homogenizer
355 Potter-Elvehjem with 60 μL of extraction buffer (0.35 M Tris-HCl (pH 6.8), 30% (v/v) glycerol, 10% (v/v) SDS,
356 0.6 M DTT, 0.012% (w/v) bromophenol blue). Total protein extracts were denatured for 7 min at 95°C,
357 centrifuged at 11 000g for 5 min and 30 μL of supernatant were separated by 12% SDS-PAGE.
358 Phosphorylation state of MAPKs by immunoblotting was performed as previously described (46).

359

360 **Depletion binding assay.** Protein expression and ligand depletion were performed as described (85) with
361 slight modifications. Briefly, LORE extracellular domain mCherry fusion protein (eLORE-mCherry) or mCherry
362 control fused with N-terminal LORE signal peptide were transiently expressed in *N. benthamiana* leaf apoplast
363 using a 1:1 mixture of *Agrobacterium tumefaciens* GV3101 carrying the respective expression plasmid or the
364 p19 silencing suppressor (total OD₆₀₀ 0.5). Five days post inoculation, *N. benthamiana* leaves were vacuum-
365 infiltrated with water and apoplastic washing fluid (AWF) was collected by centrifugation (20 min, 800 g, 4°C).
366 AWF was cleared by centrifugation (20 min, 8000 g, 4°C), filter-sterilized (pore size 0.22 μm), desalted (PD-10
367 Desalting Columns, Cytiva), and concentrated to a total protein concentration of 2 mg/mL (Vivaspin 20,
368 30 000 Da MW cut-off, Sartorius). For ligand depletion assay, AWF concentrate was mixed in 9:1 ratio (v:v)
369 with synthetic C₁₀-C₁₀ (50 μM) or 3-OH-C₁₀ (5 μM) and incubated for one hour at 4°C on a rotator. Unbound
370 ligands were separated from the mixture (Vivaspin 500, 30 000 MW cut-off, Sartorius). Content of unbound
371 C₁₀-C₁₀ and 3-OH-C₁₀ in filtrates was assessed by $[\text{Ca}^{2+}]_{\text{cyt}}$ measurements using LORE overexpressing
372 (*p35S:LORE/lore-1*) and *lore-1* seedlings with a filtrate:water ratio of 1:4 (v:v).

373

374 **Conductivity assay.** The assay was performed as described previously (83), with few modifications. Eight
375 leaf discs of 6-mm-diameter were incubated in distilled water overnight. One disc was transferred into 1.5 mL
376 tube containing fresh distilled water and the corresponding elicitor concentration or ethanol for control.
377 Conductivity measurements (three to four replicates for each treatment) were then conducted using a B-771
378 LaquaTwin (Horiba) conductivity meter.

379
380 ***Pseudomonas syringae* culture and disease resistance assays.** *Pseudomonas syringae* pv. *tomato* strain
381 DC3000 was grown at 28°C under stirring in King's B (KB) liquid medium supplemented with antibiotics: 50 µg
382 mL⁻¹ of rifampicin and 50 µg mL⁻¹ of kanamycin. For local protection assays, 15 seeds were sown per pot and
383 grown for 3 to 5 weeks in soil. Plants were sprayed with molecules or ethanol as control and were placed two
384 days in high humidity atmosphere before infections. Plants were inoculated by spraying the leaves with 3 mL
385 of a bacterial suspension at an optical density (OD₆₀₀) of 0.01 (0.025 % Silwet L-77, 10 mM MgCl₂). For each
386 experiment, 5 pots per conditions were used (n=5). Quantification (colony forming units) of *in planta* bacterial
387 growth was performed 3 dpi. To this end, all plant leaves from the same pot were harvested, weighed, and
388 crushed in a mortar with 10 mL of 10 mM MgCl₂ and serial dilutions were performed. For each dilution, 10 µL
389 were dropped on KB plate supplemented with appropriate antibiotics. Colony forming units (CFU) were
390 counted after 2 days of incubation at 28°C. The number of bacteria per mg of plants fresh mass was obtained
391 with the formula:

392

$$\text{CFU.mg}^{-1} = \frac{\left(\frac{N \times V_d}{V_i} \times 10^{(n-1)} \times 100 \right)}{M}$$

393
394 with N equal to CFU number, V_i the volume depot on plate, V_d the total volume, n the dilution number and M
395 the plants fresh mass.

396
397 **References**

- 398 1. D. E. Cook, C. H. Mesarich, B. P. Thomma, Understanding plant immunity as a surveillance system to
399 detect invasion. *Annu. Rev. Phytopathol.* **53**, 541-563 (2015).
- 400 2. K. Kanyuka, J. J. Rudd, Cell surface immune receptors: the guardians of the plant's extracellular
401 spaces. *Curr. Opin. Plant Biol.* **50**, 1-8 (2019).
- 402 3. T. Boller, G. Felix, A renaissance of elicitors: perception of microbe-associated molecular patterns
403 and danger signals by pattern-recognition receptors. *Annu. Rev. Plant Biol.* **60**, 379-406 (2009).
- 404 4. M. A. Newman, T. Sundelin, J. T. Nielsen, G. Erbs, MAMP (microbe-associated molecular pattern)
405 triggered immunity in plants. *Front. Plant Sci.* **4**, 139 (2013).
- 406 5. F. Boutrot, C. Zipfel, Function, discovery, and exploitation of plant pattern recognition receptors for
407 broad-spectrum disease resistance. *Annu. Rev. Phytopathol.* **55**, 257-286 (2017).
- 408 6. S. Ranf, Sensing of molecular patterns through cell surface immune receptors. *Curr. Opin. Plant Biol.*
409 **38**, 68-77 (2017).
- 410 7. D. Couto, C. Zipfel, Regulation of pattern recognition receptor signalling in plants. *Nat. Rev. Immunol.*
411 **16**, 537-552 (2016).
- 412 8. J. Bigeard, J. Colcombet, H. Hirt, Signaling mechanisms in pattern-triggered immunity (PTI). *Mol.*
413 *Plant* **8**, 521-539 (2015).

- 414 9. A. Garcia-Brugger *et al.*, Early signaling events induced by elicitors of plant defenses. *Mol. Plant-Microbe Interact.* **19**, 711-724 (2006).
415
- 416 10. S. Wu, L. Shan, P. He, Microbial signature-triggered plant defense responses and early signaling
417 mechanisms. *Plant Sci.* **228**, 118-126 (2014).
- 418 11. D. De Vleeschauwer, G. Gheysen, M. Hofte, Hormone defense networking in rice: tales from a
419 different world. *Trends Plant Sci.* **18**, 555-565 (2013).
- 420 12. J. Glazebrook, Contrasting mechanisms of defense against biotrophic and necrotrophic pathogens.
421 *Annu. Rev. Phytopathol.* **43**, 205-227 (2005).
- 422 13. A. Robert-Seilaniantz, M. Grant, J. D. Jones, Hormone crosstalk in plant disease and defense: more
423 than just jasmonate-salicylate antagonism. *Annu. Rev. Phytopathol.* **49**, 317-343 (2011).
- 424 14. L. Trda *et al.*, Perception of pathogenic or beneficial bacteria and their evasion of host immunity:
425 pattern recognition receptors in the frontline. *Front. Plant Sci.* **6**, 219 (2015).
- 426 15. A. M. Abdel-Mawgoud, F. Lépine, E. Déziel, Rhamnolipids: diversity of structures, microbial origins
427 and roles. *Appl. Microbiol. Biotechnol.* **86**, 1323-1336 (2010).
- 428 16. V. U. Irorere, L. Tripathi, R. Marchant, S. McClean, I. M. Banat, Microbial rhamnolipid production: a
429 critical re-evaluation of published data and suggested future publication criteria. *Appl. Microbiol.*
430 *Biotechnol.* **101**, 3941-3951 (2017).
- 431 17. M. Perneel *et al.*, Phenazines and biosurfactants interact in the biological control of soil-borne
432 diseases caused by *Pythium* spp. *Environ. Microbiol.* **10**, 778-788 (2008).
- 433 18. L. Chrzanowski, L. Lawniczak, K. Czaczyk, Why do microorganisms produce rhamnolipids? *World J.*
434 *Microbiol. Biotechnol.* **28**, 401-419 (2012).
- 435 19. A. Nickzad, E. Déziel, The involvement of rhamnolipids in microbial cell adhesion and biofilm
436 development - an approach for control? *Letts. Appl. Microbiol.* **58**, 447-453 (2014).
- 437 20. P. Vatsa, L. Sanchez, C. Clément, F. Baillieul, S. Dorey, Rhamnolipid biosurfactants as new players
438 in animal and plant defense against microbes. *Int. J. Mol. Sci.* **11**, 5095-5108 (2010).
- 439 21. A. M. Abdel-Mawgoud, F. Lépine, E. Déziel, A stereospecific pathway diverts beta-oxidation
440 intermediates to the biosynthesis of rhamnolipid biosurfactants. *Chem. Biol.* **21**, 156-164 (2014).
- 441 22. A. Y. Burch *et al.*, *Pseudomonas syringae* coordinates production of a motility-enabling surfactant with
442 flagellar assembly. *J. Bacteriol.* **194**, 1287-1298 (2012).
- 443 23. E. Déziel, F. Lépine, S. Milot, R. Villemur, *rhlA* is required for the production of a novel biosurfactant
444 promoting swarming motility in *Pseudomonas aeruginosa*: 3-(3-hydroxyalkanoyloxy)alkanoic acids
445 (HAAs), the precursors of rhamnolipids. *Microbiology* **149**, 2005-2013 (2003).
- 446 24. J. M. Plotnikova, L. G. Rahme, F. M. Ausubel, Pathogenesis of the human opportunistic pathogen
447 *Pseudomonas aeruginosa* PA14 in *Arabidopsis*. *Plant Physiol.* **124**, 1766-1774 (2000).
- 448 25. J. Tremblay, A. P. Richardson, F. Lépine, E. Déziel, Self-produced extracellular stimuli modulate the
449 *Pseudomonas aeruginosa* swarming motility behaviour. *Environ. Microbiol.* **9**, 2622-2630 (2007).
- 450 26. U. Gerstel, M. Czapp, J. Bartels, J. M. Schroder, Rhamnolipid-induced shedding of flagellin from
451 *Pseudomonas aeruginosa* provokes hBD-2 and IL-8 response in human keratinocytes. *Cell. Microbiol.*
452 **11**, 842-853 (2009).
- 453 27. R. A. Al-Tahhan, T. R. Sandrin, A. A. Bodour, R. M. Maier, Rhamnolipid-induced removal of
454 lipopolysaccharide from *Pseudomonas aeruginosa*: effect on cell surface properties and interaction
455 with hydrophobic substrates. *Appl. Environ. Microbiol.* **66**, 3262-3268 (2000).
- 456 28. J. Andrä *et al.*, Endotoxin-like properties of a rhamnolipid exotoxin from *Burkholderia (Pseudomonas)*
457 *plantarii*: immune cell stimulation and biophysical characterization. *Biol. Chem.* **387**, 301-310 (2006).
- 458 29. J. Bauer, K. Brandenburg, U. Zahringer, J. Rademann, Chemical synthesis of a glycolipid library by a
459 solid-phase strategy allows elucidation of the structural specificity of immunostimulation by
460 rhamnolipids. *Chemistry* **12**, 7116-7124 (2006).

- 461 30. J. Dossel, U. Meyer-Hoffert, J. M. Schroder, U. Gerstel, *Pseudomonas aeruginosa*-derived
462 rhamnolipids subvert the host innate immune response through manipulation of the human beta-
463 defensin-2 expression. *Cell. Microbiol.* **14**, 1364-1375 (2012).
- 464 31. M. Gonzalez-Juarrero *et al.*, Polar lipids of *Burkholderia pseudomallei* induce different host immune
465 responses. *PLoS one* **8**, e80368 (2013).
- 466 32. L. Sanchez *et al.*, Rhamnolipids elicit defense responses and induce disease resistance against
467 biotrophic, hemibiotrophic, and necrotrophic pathogens that require different signaling pathways in
468 *Arabidopsis* and highlight a central role for salicylic acid. *Plant Physiol.* **160**, 1630-1641 (2012).
- 469 33. A. L. Varnier *et al.*, Bacterial rhamnolipids are novel MAMPs conferring resistance to *Botrytis cinerea*
470 in grapevine. *Plant, Cell Environ.* **32**, 178-193 (2009).
- 471 34. A. Kutschera *et al.*, Bacterial medium-chain 3-hydroxy fatty acid metabolites trigger immunity in
472 *Arabidopsis* plants. *Science* **364**, 178-181 (2019).
- 473 35. J. Qi, J. Wang, Z. Gong, J. M. Zhou, Apoplastic ROS signaling in plant immunity. *Curr. Opin. Plant*
474 *Biol.* **38**, 92-100 (2017).
- 475 36. Y. Kadota, K. Shirasu, C. Zipfel, Regulation of the NADPH oxidase RBOHD during plant immunity.
476 *Plant Cell Physiol.* **56**, 1472-1480 (2015).
- 477 37. M. A. Torres, J. L. Dangl, J. D. Jones, *Arabidopsis* gp91phox homologues AtrbohD and AtrbohF are
478 required for accumulation of reactive oxygen intermediates in the plant defense response. *Proc. Natl.*
479 *Acad. Sci. USA* **99**, 517-522 (2002).
- 480 38. D. Chinchilla, Z. Bauer, M. Regenass, T. Boller, G. Felix, The *Arabidopsis* receptor kinase FLS2 binds
481 flg22 and determines the specificity of flagellin perception. *Plant Cell* **18**, 465-476 (2006).
- 482 39. C. Zipfel *et al.*, Perception of the bacterial PAMP EF-Tu by the receptor EFR restricts *Agrobacterium*-
483 mediated transformation. *Cell* **125**, 749-760 (2006).
- 484 40. M. Roux *et al.*, The *Arabidopsis* leucine-rich repeat receptor-like kinases BAK1/SERK3 and
485 BKK1/SERK4 are required for innate immunity to hemibiotrophic and biotrophic pathogens. *Plant Cell*
486 **23**, 2440-2455 (2011).
- 487 41. L. Li *et al.*, The FLS2-associated kinase BIK1 directly phosphorylates the NADPH oxidase RbohD to
488 control plant immunity. *Cell Host Microbe* **15**, 329-338 (2014).
- 489 42. A. Miya *et al.*, CERK1, a LysM receptor kinase, is essential for chitin elicitor signaling in *Arabidopsis*.
490 *Proc. Natl. Acad. Sci. USA* **104**, 19613-19618 (2007).
- 491 43. W. Zhang *et al.*, *Arabidopsis* receptor-like protein30 and receptor-like kinase suppressor of BIR1-
492 1/EVERSHED mediate innate immunity to necrotrophic fungi. *Plant Cell* **25**, 4227-4241 (2013).
- 493 44. J. Choi *et al.*, Identification of a plant receptor for extracellular ATP. *Science* **343**, 290-294 (2014).
- 494 45. S. Ranf *et al.*, A lectin S-domain receptor kinase mediates lipopolysaccharide sensing in *Arabidopsis*
495 *thaliana*. *Nat. Immunol.* **16**, 426-433 (2015).
- 496 46. P. Luzuriaga-Loaiza *et al.*, Synthetic rhamnolipid bolafoms trigger an innate immune response in
497 *Arabidopsis thaliana*. *Sci. Rep.* **8**, 8534 (2018).
- 498 47. K. Shang-Guan *et al.*, Lipopolysaccharides trigger two successive bursts of reactive oxygen species
499 at distinct cellular locations. *Plant Physiol.* **176**, 2543-2556 (2018).
- 500 48. X. F. Xin, S. Y. He, *Pseudomonas syringae* pv. *tomato* DC3000: a model pathogen for probing
501 disease susceptibility and hormone signaling in plants. *Annu. Rev. Phytopathol.* **51**, 473-498 (2013).
- 502 49. S. G. Costa, E. Déziel, F. Lépine, Characterization of rhamnolipid production by *Burkholderia glumae*.
503 *Lett. Appl. Microbiol.* **53**, 620-627 (2011).
- 504 50. J. H. Ham, R. A. Melanson, M. C. Rush, *Burkholderia glumae*: next major pathogen of rice? *Mol. Plant*
505 *Pathol.* **12**, 329-339 (2011).
- 506 51. A. B. Stephan, H. H. Kunz, E. Yang, J. I. Schroeder, Rapid hyperosmotic-induced Ca²⁺ responses in
507 *Arabidopsis thaliana* exhibit sensory potentiation and involvement of plastidial KEA transporters. *Proc.*
508 *Natl. Acad. Sci. USA* **113**, E5242-5249 (2016).

- 509 52. T. Lenarcic *et al.*, Eudicot plant-specific sphingolipids determine host selectivity of microbial NLP
510 cytolysins. *Science* **358**, 1431-1434 (2017).
- 511 53. N. C. Caiazza, R. M. Shanks, G. A. O'Toole, Rhamnolipids modulate swarming motility patterns of
512 *Pseudomonas aeruginosa*. *J. Bacteriol.* **187**, 7351-7361 (2005).
- 513 54. A. Nickzad, F. Lépine, E. Déziel, Quorum sensing controls swarming motility of *Burkholderia glumae*
514 through regulation of rhamnolipids. *PLoS one* **10**, e0128509 (2015).
- 515 55. X. Yu *et al.*, Transcriptional responses of *Pseudomonas syringae* to growth in epiphytic versus
516 apoplastic leaf sites. *Proc. Natl. Acad. Sci. USA* **110**, E425-434 (2013).
- 517 56. M. E. Davey, N. C. Caiazza, G. A. O'Toole, Rhamnolipid surfactant production affects biofilm
518 architecture in *Pseudomonas aeruginosa* PAO1. *J. Bacteriol.* **185**, 1027-1036 (2003).
- 519 57. H. Hirai *et al.*, Glycosylation regulates specific induction of rice immune responses by *Acidovorax*
520 *avenae* flagellin. *J. Biol. Chem.* **286**, 25519-25530 (2011).
- 521 58. F. Taguchi *et al.*, Glycosylation of flagellin from *Pseudomonas syringae* pv. tabaci 6605 contributes to
522 evasion of host tobacco plant surveillance system. *Physiol. Mol. Plant Pathol.* **74**, 11-17 (2009).
- 523 59. A. Hanuszkiewicz *et al.*, Identification of the flagellin glycosylation system in *Burkholderia*
524 *cenocepacia* and the contribution of glycosylated flagellin to evasion of human innate immune
525 responses. *J. Biol. Chem.* **289**, 19231-19244 (2014).
- 526 60. G. Henry, M. Deleu, E. Jourdan, P. Thonart, M. Ongena, The bacterial lipopeptide surfactin targets
527 the lipid fraction of the plant plasma membrane to trigger immune-related defence responses. *Cell.*
528 *Microbiol.* **13**, 1824-1837 (2011).
- 529 61. M. N. Nasir *et al.*, Differential interaction of synthetic glycolipids with biomimetic plasma membrane
530 lipids correlates with the plant biological response. *Langmuir* **33**, 9979-9987 (2017).
- 531 62. M. Robineau *et al.*, Synthetic mono-rhamnolipids display direct antifungal effects and trigger an innate
532 immune response in tomato against *Botrytis cinerea*. *Molecules* **25**, 3108 (2020).
- 533 63. H. Abbasi, K. A. Noghbi, A. Ortiz, Interaction of a bacterial monorhamnolipid secreted by
534 *Pseudomonas aeruginosa* MA01 with phosphatidylcholine model membranes. *Chem. Phys. Lipids*
535 **165**, 745-752 (2012).
- 536 64. F. J. Aranda *et al.*, Thermodynamics of the interaction of a dirhamnolipid biosurfactant secreted by
537 *Pseudomonas aeruginosa* with phospholipid membranes. *Langmuir* **23**, 2700-2705 (2007).
- 538 65. A. Ortiz, F. J. Aranda, J. A. Teruel, Interaction of dirhamnolipid biosurfactants with phospholipid
539 membranes: a molecular level study. *Adv. Exp. Med. Biol.* **672**, 42-53 (2010).
- 540 66. M. Sanchez, F. J. Aranda, J. A. Teruel, A. Ortiz, Interaction of a bacterial dirhamnolipid with
541 phosphatidylcholine membranes: a biophysical study. *Chem. Phys. Lipids* **161**, 51-55 (2009).
- 542 67. N. Monnier *et al.*, Exploring the dual interaction of natural rhamnolipids with plant and fungal
543 biomimetic plasma membranes through biophysical studies. *Int. J. Mol. Sci.* **20**, 1009 (2019).
- 544 68. F. Lépine, E. Déziel, S. Milot, R. Villemur, Liquid chromatographic/mass spectrometric detection of the
545 3-(3-hydroxyalkanoyloxy) alkanolic acid precursors of rhamnolipids in *Pseudomonas aeruginosa*
546 cultures. *J. Mass Spectrom.* **37**, 41-46 (2002).
- 547 69. R. Kohnatzki, B. Tummler, G. Doring, Rhamnolipid of *Pseudomonas aeruginosa* in sputum of cystic
548 fibrosis patients. *Lancet* **1**, 1026-1027 (1987).
- 549 70. R. C. Read *et al.*, Effect of *Pseudomonas aeruginosa* rhamnolipids on mucociliary transport and
550 ciliary beating. *J. Appl. Physiol.* **72**, 2271-2277 (1992).
- 551 71. M. Somerville *et al.*, Release of mucus glycoconjugates by *Pseudomonas aeruginosa* rhamnolipid into
552 feline trachea *in vivo* and human bronchus *in vitro*. *Am. J. Respir. Cell Mol. Biol.* **6**, 116-122 (1992).
- 553 72. A. Germer *et al.*, Exploiting the natural diversity of RhIA acyltransferases for the synthesis of the
554 rhamnolipid precursor 3-(3-Hydroxyalkanoyloxy)alkanoic acid. *Appl. Environ. Microbiol.* **86**, e02317-
555 02319 (2020).
- 556 73. S. Ranf, Immune sensing of lipopolysaccharide in plants and animals: same but different. *PLOS*
557 *Pathog.* **12**, e1005596 (2016).

- 558 74. S. Compant, J. Nowak, T. Coenye, C. Clément, E. Ait Barka, Diversity and occurrence of *Burkholderia*
559 spp. in the natural environment. *FEMS Microbiol. Rev.* **32**, 607-626 (2008).
- 560 75. E. Kay, F. Bertolla, T. M. Vogel, P. Simonet, Opportunistic colonization of *Ralstonia solanacearum*-
561 infected plants by *Acinetobacter* sp. and its natural competence development. *Microb. Ecol.* **43**, 291-
562 297 (2002).
- 563 76. M. W. Silby, C. Winstanley, S. A. Godfrey, S. B. Levy, R. W. Jackson, *Pseudomonas* genomes:
564 diverse and adaptable. *FEMS Microbiol. Rev.* **35**, 652-680 (2011).
- 565 77. I. K. Toth, L. Pritchard, P. R. J. Birch, Comparative genomics reveals what makes an enterobacterial
566 plant pathogen. *Annu. Rev. Phytopathol.* **44**, 305-336 (2006).
- 567 78. X. Yu *et al.*, Transcriptional analysis of the global regulatory networks active in *Pseudomonas*
568 *syringae* during leaf colonization. *mBio* **5**, e01683-01614 (2014).
- 569 79. K. Zhu, C. O. Rock, RhIA converts beta-hydroxyacyl-acyl carrier protein intermediates in fatty acid
570 synthesis to the beta-hydroxydecanoyl-beta-hydroxydecanoate component of rhamnolipids in
571 *Pseudomonas aeruginosa*. *J. Bacteriol.* **190**, 3147-3154 (2008).
- 572 80. P. Buscaill *et al.*, Glycosidase and glycan polymorphism control hydrolytic release of immunogenic
573 flagellin peptides. *Science* **364**, eaav0748 (2019).
- 574 81. F. Taguchi *et al.*, Effects of glycosylation on swimming ability and flagellar polymorphic transformation
575 in *Pseudomonas syringae* pv. *tabaci* 6605. *J. Bacteriol.* **190**, 764-768 (2008).
- 576 82. J. M. Smith, A. Heese, Rapid bioassay to measure early reactive oxygen species production in
577 *Arabidopsis* leave tissue in response to living *Pseudomonas syringae*. *Plant Methods* **10**, 6 (2014).
- 578 83. M. Magnin-Robert *et al.*, Modifications of sphingolipid content affect tolerance to hemibiotrophic and
579 necrotrophic pathogens by modulating plant defense responses in *Arabidopsis*. *Plant Physiol.* **169**,
580 2255-2274 (2015).
- 581 84. M. De Vleeschouwer *et al.*, Rapid total synthesis of cyclic lipodepsipeptides as a premise to
582 investigate their self-assembly and biological activity. *Chem. Eur. J.* **20**, 7766-7775 (2014).
- 583 85. L. J. Shu *et al.*, Low cost, medium throughput depletion-binding assay for screening S-domain-
584 receptor ligand interactions using in planta protein expression. *bioRxiv* doi:
585 10.1101/2021.06.16.448648 (2021).
- 586 86. König *et al.*, *Arabidopsis* mutants of sphingolipid fatty acid α -hydroxylases accumulate ceramides and
587 salicylates. *New Phytol.* **196**, 1086-1097 (2012).

588

589

590 **Acknowledgments**

591

592

593

594

595

596

597

598

Author contributions

599

600

601

602

J.C. and S.D. designed the research; R.S., J.C., L.J.S, A.K., T.G., M.T., S.V., S.D.C. performed the experiments; A.N. and E.D. purified and characterized HAAs and *B. glumae* RLs; M.C. and C.G. chemically synthesized HAAs; N.B., J.H., A.H. and J.H.R., purified *P. aeruginosa* RLs; C.D. and C.S. quantified mc-3-OH-FAs in all samples; R.S., J.C., L.J.S, S.C., F.M.G., F.B., S.R., E.D. and S.D. analyzed the data; R.S., J.C. and

603 S.D. wrote the manuscript. M.O., J.H.R., A.H., T.H., C.Z., F.B., C.C., S.R and E.D contributed ideas, and
604 critically revised the manuscript. All authors discussed the results and approved the manuscript.

605

606 **Additional Information**

607

608 **Data availability**

609 The authors declare that all data supporting the findings of this study can be found within the
610 manuscript and its Supplementary Files.

611

612 **Competing financial interests**

613 Technical University of Munich has filed a patent application to inventors A.K., C.D., T.H., and S.R.
614 The authors declare no financial conflicts of interest in relation to this work.
615 All other author(s) declare no competing financial and/or non-financial interests.

616

617

618 **Figure legends**

619

620 **Fig. 1. RLsec activates LORE-dependent early immune-related responses in *Arabidopsis*.** (A)
621 Extracellular ROS production after treatment of WT leaf petioles with 50 µg/mL RLsec or EtOH as control. (B)
622 Dose effect of RLsec on ROS production. ROS production measured after treatment of WT leaf petioles with
623 the indicated concentrations of RLsec or EtOH as control. (C) ROS production measured after treatment of
624 WT, *fls2/efr1*, *dorn1-1*, *bak1-5*, *bkk1-1*, *bak1-5/bkk1-1*, *cerk1-2*, *sobir1-12*, *sobir1-13*, *bik1/pbl1*, *lore-5*, or
625 *rbohD* leaf petioles with 50 µg/mL RLsec. (A-C) Data are mean ± SEM (n = 6). (A-C) Experiments have been
626 realized three times with similar results.

627

628 **Fig. 2. RLsec activates LORE-independent responses in *Arabidopsis*.** (A) Extracellular ROS production
629 after treatment of WT, *lore-5*, and *rbohD* leaf petioles with 50 µg/mL RLsec or EtOH (Control). ROS
630 production was monitored over 720 minutes. Data are mean ± SEM (n = 6). Experiments have been realized
631 three times with similar results. (B) WT (red) and *lore-5* (blue) *Arabidopsis* leaves were treated with 50 µg/mL
632 RLsec (triangle) or EtOH (square) (control) 48 h before infection. *Pst* titers were measured at 3 d.p.i. Data are
633 individual data and mean (black line) (n = 5). Experiments have been realized three times with similar results.
634 Letters represent results of pairwise Welch statistic test with Bonferroni correction with $P > 0.05$ (same letters)
635 or $P \leq 0.05$ (different letters).

636

637 **Fig. 3. Purified HAAs from *P. aeruginosa* trigger a LORE-dependent immune response in *Arabidopsis*.**
638 (A) Dose effect of 3-OH-C₁₀ and C₁₀-C₁₀ purified from *P. aeruginosa* on ROS production by WT leaf petioles.
639 EtOH was used as negative control. Data are mean ± SEM (n = 6). Experiments have been realized twice with
640 similar results. (B) Maximum (Max.) increases in [Ca²⁺]_{cyt} in *Arabidopsis* Col-0^{AEQ} seedlings treated with
641 different concentrations of 3-OH-C₁₀, C₁₀-C₁₀ purified from *P. aeruginosa* or MeOH as control. Data are mean
642 ± SD (n = 3). Experiments have been realized twice with similar results. (C) ROS production measured after

643 treatment of WT, *lore-5*, or *rbohD* leaf petioles with 10 μM 3-OH-C₁₀, 10 μM purified C₁₀-C₁₀ or EtOH as
644 control. Data are mean \pm SEM (n = 6). Experiments have been realized three times with similar results. (D)
645 Maximum (Max.) increases in [Ca²⁺]_{cyt} in *Arabidopsis* Col-0^{AEQ} and *lore-5*^{AEQ} seedlings treated with 5 μM 3-
646 OH-C₁₀ or purified C₁₀-C₁₀. Data are mean \pm SD (n = 3). Experiments have been realized twice with similar
647 results. For B and D, the same Col-0^{AEQ} 5 μM data are presented (same experiments). (E) WT (red) and *lore*-
648 5 (blue) *Arabidopsis* leaves were treated with 10 μM 3-OH-C₁₀ (triangle), 10 μM purified C₁₀-C₁₀ (diamond) or
649 EtOH (square) (control) 48 h before infection. *Pst* titers were measured at 3 d.p.i. Data are individual data and
650 mean (black line) (n = 5). Experiments have been realized twice with similar results. Letters represent results
651 of pairwise Welch statistic test with Bonferroni correction with $P > 0.05$ (same letters) or $P \leq 0.05$ (different
652 letters).

653

654 **Fig. 4. Synthetic HAAs trigger a LORE-dependent immune response in *Arabidopsis*.** (A) Maximum
655 (Max.) increases in [Ca²⁺]_{cyt} in *Arabidopsis* Col-0^{AEQ} seedlings treated with different concentrations of 3-OH-
656 C₁₀, synthetic C₁₀-C₁₀ or MeOH. Data are mean \pm SD (n = 3). Experiments have been realized twice with
657 similar results. (B) Dose effect of synthetic C₁₀-C₁₀ on ROS production by WT leaf petioles. EtOH was used as
658 negative control. Data are mean \pm SEM (n = 6). Experiments have been realized twice with similar results. (C)
659 Maximum (Max.) increases in [Ca²⁺]_{cyt} in *Arabidopsis* Col-0^{AEQ} and *lore-5*^{AEQ} seedlings treated with 5 μM 3-
660 OH-C₁₀ or synthetic C₁₀-C₁₀. Data are mean \pm SD (n = 3). Experiments have been realized twice with similar
661 results. (D) WT (red) and *lore-5* (blue) *Arabidopsis* leaves were treated with 10 μM 3-OH-C₁₀ (triangle), 10 μM
662 synthetic C₁₀-C₁₀ (diamond), or MeOH (square) (control) 48 h before infection. *Pst* titers were measured at 3
663 d.p.i. Data are individual data and mean (black line) (n = 5). Experiments have been realized twice with similar
664 results. Letters represent data of pairwise Welch statistic test with Bonferroni correction with $P > 0.05$ (same
665 letters) or $P \leq 0.05$ (different letters). (E) Depletion of 1 μM synthetic C₁₀-C₁₀ or 100 nM 3-OH-C₁₀ by
666 concentrated apoplastic wash fluid from *Nicotiana benthamiana* containing LORE extracellular domain
667 (eLORE)-mCherry fusion protein or apoplastic (apo)-mCherry as control as illustrated in supplemental figure
668 8A. Unbound ligand content in low-molecular-weight filtrate was analyzed by [Ca²⁺]_{cyt} measurements in LORE-
669 overexpressing (OE; red bars, grey triangles, n = 12) and *lore-1* (blue bars, grey diamonds, n = 6) *Arabidopsis*
670 seedlings. Data are mean \pm SD and individual data of three pooled experiments. Letters represent data of
671 pairwise Wilcoxon statistic test with Bonferroni correction with $P > 0.05$ (same letters) or $P \leq 0.05$ (different
672 letters).

673

674 **Fig. 5. Purified RLs trigger a LORE-independent *Arabidopsis* immune response.** (A) Extracellular late
675 ROS production after treatment of WT leaf petioles with 100 μM RLs, 100 μM L-rhamnose, or EtOH (control).
676 Data are mean \pm SEM (n = 6). (B) Dose effect of Rha-Rha-C₁₀-C₁₀ on late ROS production. ROS production
677 measured after treatment of WT leaf petioles with the indicated concentrations of Rha-Rha-C₁₀-C₁₀ or EtOH
678 (control). Data are mean \pm SEM (n = 6). (C) Late ROS production measured after treatment of WT, *lore-5*, or
679 *rbohD* leaf petioles with 100 μM Rha-Rha-C₁₀-C₁₀. Data are mean \pm SEM (n = 6). (D) WT (red) and *lore-5*
680 (blue) *Arabidopsis* leaves were treated with 10 μM Rha-Rha-C₁₀-C₁₀ (triangle) or EtOH (square) (control) 48 h
681 before infection. *Pst* titers were measured at 3 d.p.i. Data are individual data and mean (black line) (n = 5).

682 Letters represent results of pairwise t statistic test with Bonferroni correction with $P > 0.05$ (same letters) or P
683 ≤ 0.05 (different letters). (A-D) Experiments have been realized three times with similar results.

684

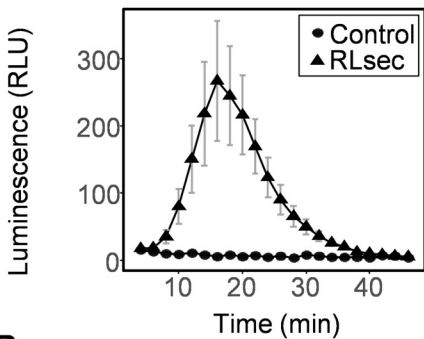
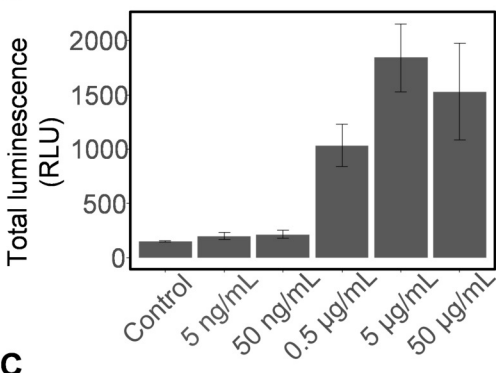
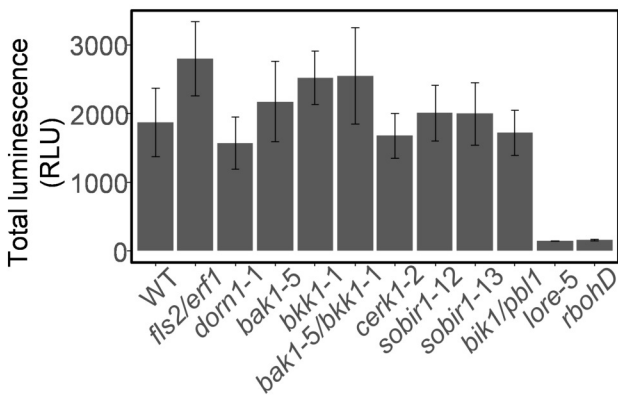
685 **Fig. 6. RL perception is impacted by plasma membrane sphingolipid composition.** Extracellular late
686 ROS production after treatment of (A) WT, *cerk1-2*, *dorn1-1*, *sobir1-12*, *bak1-5/bkk1-1*, *bik1/pbl1*, *mca1/2*,
687 *msl4/5/6/9/10* (*msl*), or *rbohD*, and (B) WT, *loh1*, or *fah1/2* *Arabidopsis* leaf petioles with 100 μ M Rha-Rha-
688 C₁₀-C₁₀ or EtOH (control). Data are mean \pm SEM ($n = 6$). Experiments have been realized three times with
689 similar results. (C) Electrolyte leakage induced by 100 μ M Rha-C₁₀-C₁₀ or EtOH (Control) on WT, *loh1*, or
690 *fah1/2* *Arabidopsis* leaf discs 24h post treatment. Data are mean \pm SEM ($n = 6$). Letters represent results of
691 pairwise Wilcoxon-Mann-Whitney statistic test with $P > 0.05$ (same letters) or $P \leq 0.05$ (different letters).
692 Experiments have been realized twice with similar results. (D) WT (red) and *fah1/2* (blue) *Arabidopsis* leaves
693 were treated with 10 μ M Rha-C₁₀-C₁₀ (triangle) or EtOH (square) (control) 48 h before infection. *Pst* titers were
694 measured at 3 d.p.i. Data are individual data and mean (black line) ($n = 5$). Letters represent results of
695 pairwise Welch statistic test with Bonferroni correction with $P > 0.05$ (same letters) or $P \leq 0.05$ (different
696 letters).

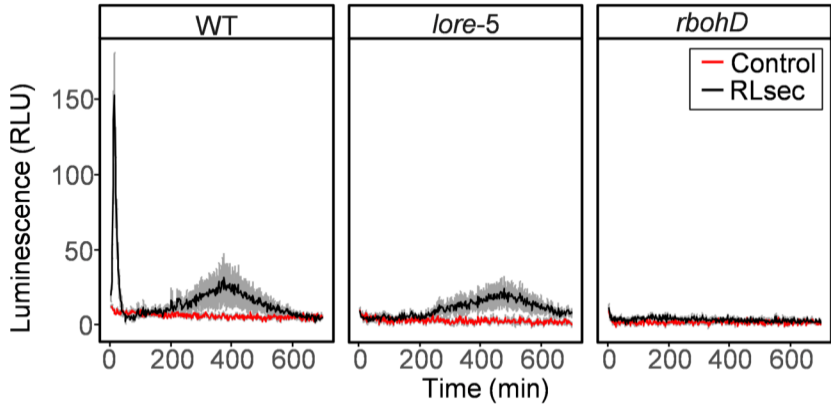
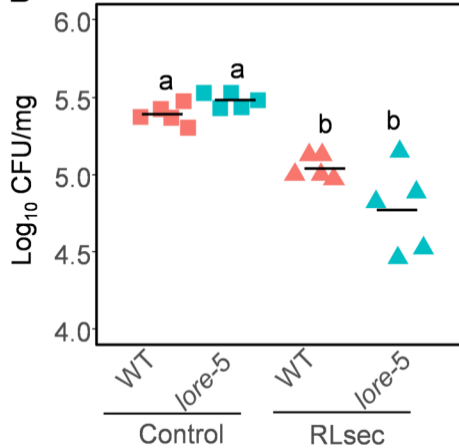
697

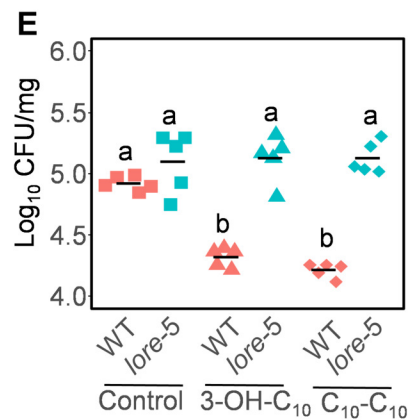
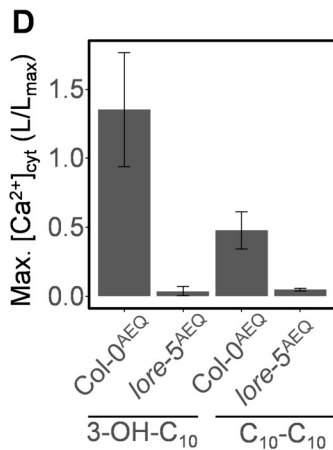
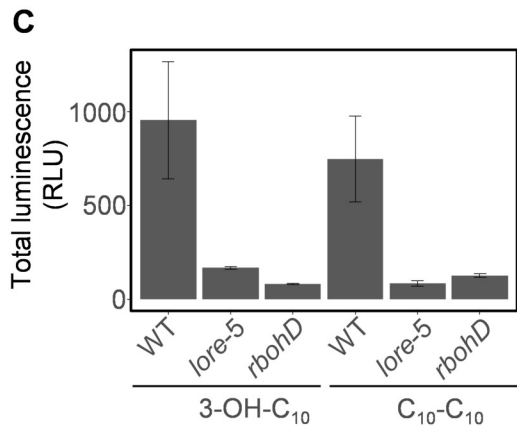
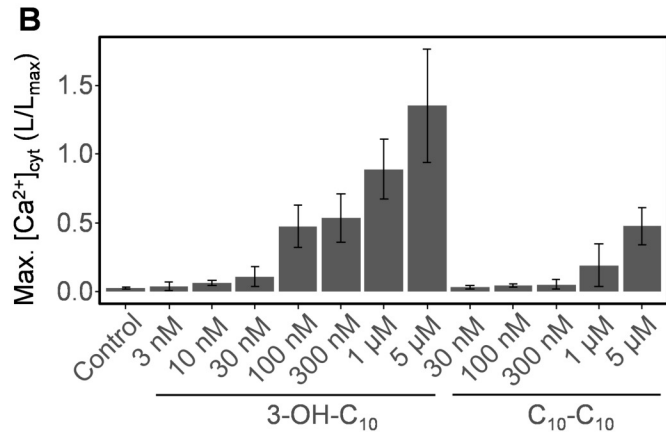
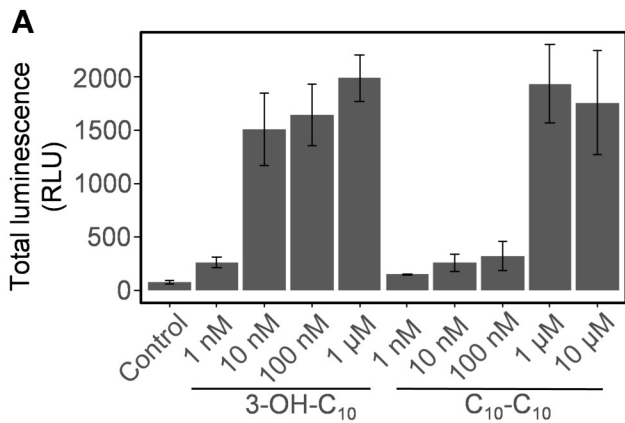
698 **Fig. 7: Proposed model for HAA and rhamnolipid perception mechanisms in *Arabidopsis* and**
699 **integrated immune responses.** RL-producing bacteria excrete rhamnolipids and HAAs to form biofilm and
700 for successful colonization. *Arabidopsis* perceives HAAs *via* LORE and rhamnolipids by a LORE-independent
701 pathway affected by sphingolipids composition of the plant plasma membrane, resulting in the activation of
702 efficient immune responses. Parts of this scheme were created with BioRender.com.

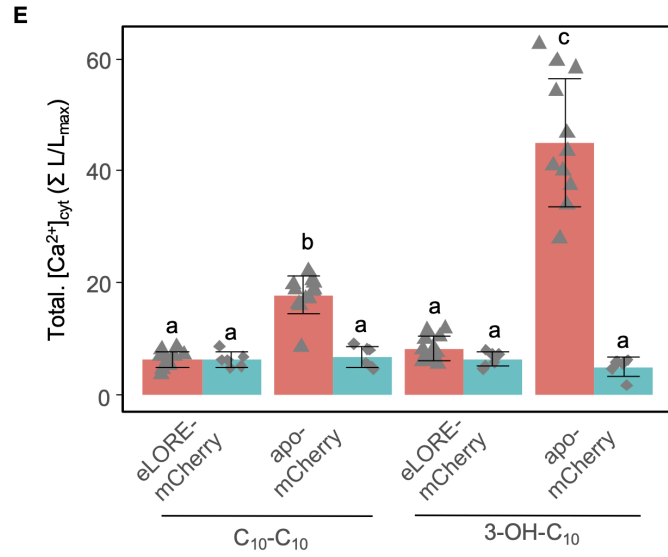
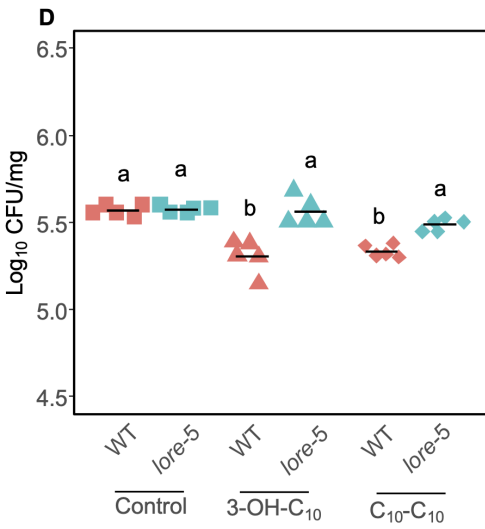
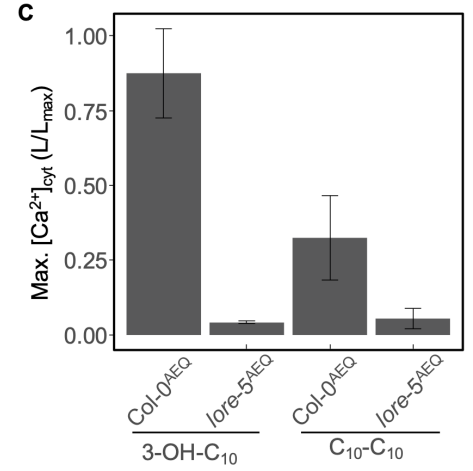
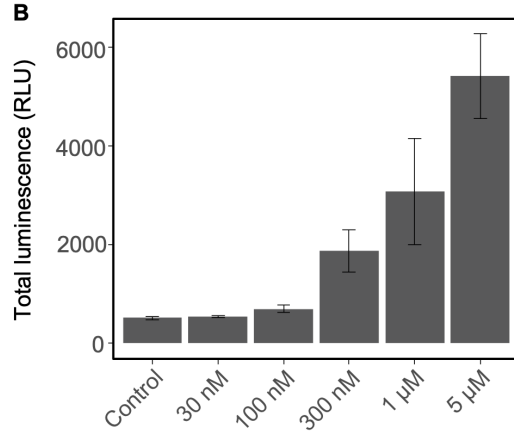
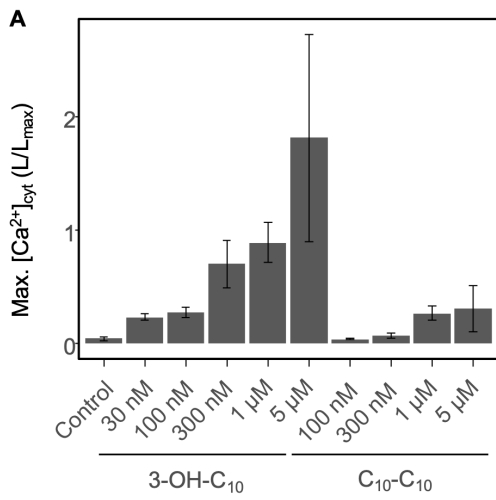
703

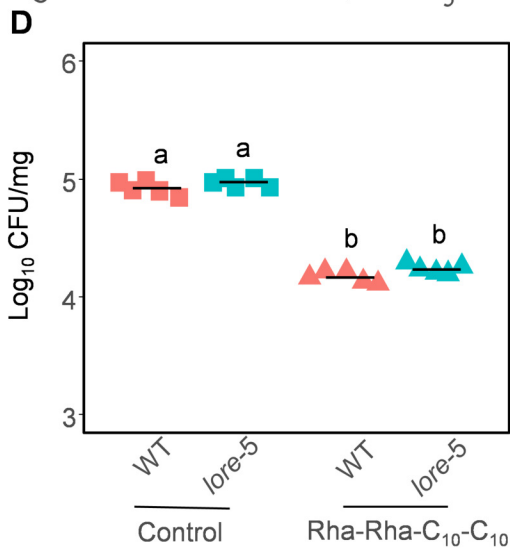
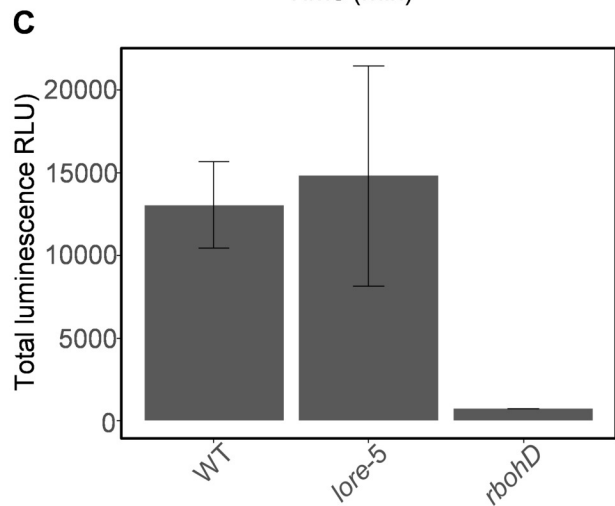
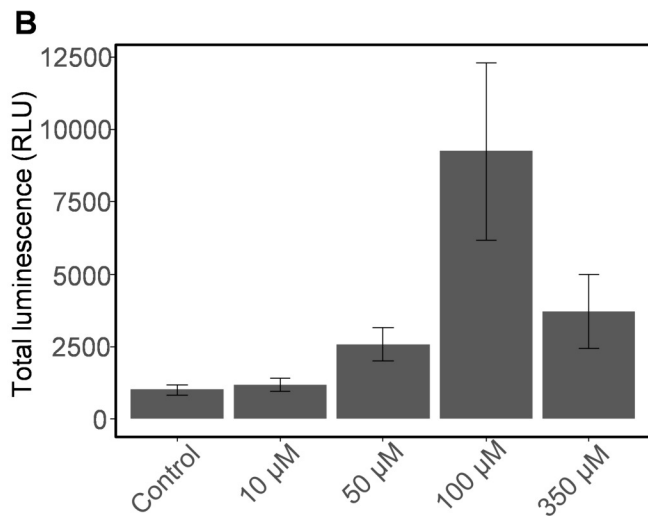
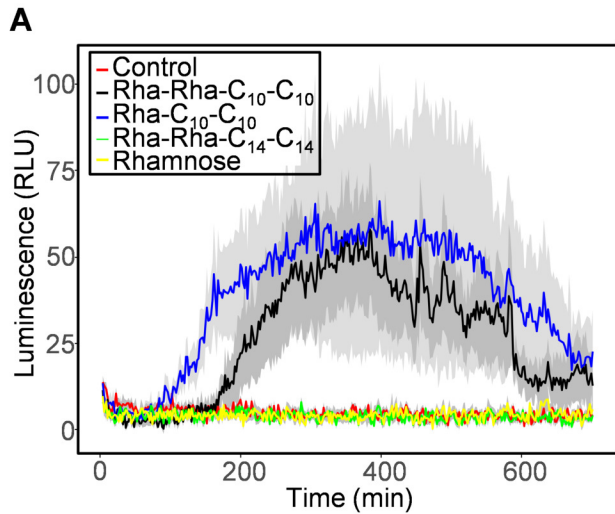
704

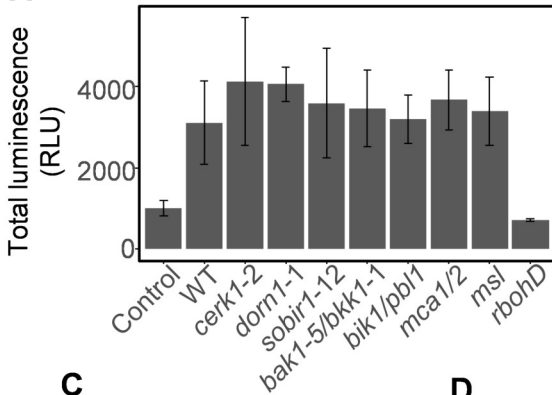
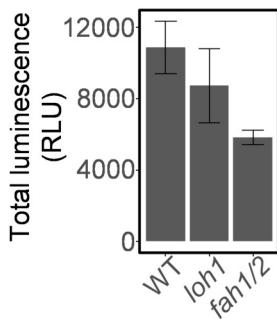
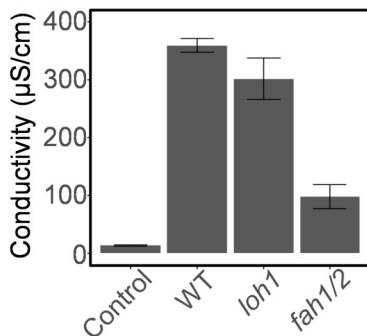
A**B****C**

A**B**







A**B****C****D**